

Immunogenicity and Reactivity of Novel *Mycobacterium avium* subsp. *paratuberculosis* PPE MAP1152 and Conserved MAP1156 Proteins with Sera from Experimentally and Naturally Infected Animals^{∇†}

John P. Bannantine,¹ Avery L. Paulson,² Ofelia Chacon,² Robert J. Fenton,² Denise K. Zinniel,² David S. McVey,² David R. Smith,² Charles J. Czuprynski,³ and Raúl G. Barletta^{2*}

Bacterial Diseases of Livestock Research Unit, USDA ARS National Animal Disease Center, Ames, Iowa 50010¹; School of Veterinary Medicine and Biomedical Sciences, University of Nebraska, Lincoln, Nebraska 68583²; and Department of Pathobiological Sciences, School of Veterinary Medicine, University of Wisconsin—Madison, Madison, Wisconsin 53706³

Received 23 July 2010/Returned for modification 13 September 2010/Accepted 9 November 2010

Mycobacterium avium subsp. *paratuberculosis* causes Johne's disease (JD) in ruminants. Development of genetic tools and completion of the *M. avium* subsp. *paratuberculosis* genome sequencing project have expanded the opportunities for antigen discovery. In this study, we determined the seroreactivities of two proteins encoded at the 5' and 3' regions of the MAP1152-MAP1156 gene cluster. MAP1152 encodes a PPE protein, and MAP1156 encodes a diacylglycerol acyltransferase involved in triglyceride metabolism and classified in the uncharacterized protein family UPF0089. Recombinant MAP proteins were overproduced and purified from *Escherichia coli* as maltose-binding protein (MBP) fusions. Immunoblotting analysis indicated that both MAP1152 and MAP1156 displayed reactivity against sera of mice and rabbits immunized with live *M. avium* subsp. *paratuberculosis* cells and against samples from naturally infected cattle. In immunoblot assays, MAP1156 yielded a stronger positive signal than MAP1152 against sera from cattle with JD. An enzyme-linked immunosorbent assay for the recombinant proteins was developed and used to test preclassified positive and negative serum samples from naturally infected and noninfected cattle. Samples, with one exception, displayed no seroreactivity against the MBP-LacZ fusion protein ($P > 0.05$), the negative-control antigen. MAP1152 displayed seroreactivity against all positive sera but no seroreactivity to the negative sera ($P < 0.01$). MAP1156 displayed stronger and more variable reactivity than MAP1152, but significant differences were observed between noninfected and infected cattle ($P < 0.05$). Otherwise, degrees of reactivity followed the same trend as the positive reference antigen. In conclusion, both proteins are immunogenic in mice and rabbits, and *M. avium* subsp. *paratuberculosis*-infected cattle mount a humoral response to both MAP1152 and MAP1156 cross-reactive epitopes. These findings have potential applications to diagnostics, vaccine production, and elucidation of the immunopathogenesis of JD.

Mycobacterium avium subsp. *paratuberculosis*, one of the slowest-growing mycobacteria (28), is the etiologic agent of Johne's disease (JD) in ruminants (11, 24). JD is a chronic enteritis with significant economic impact and worldwide distribution (23, 51, 53, 57). A JD regression model estimates that losses to the dairy industry range from \$40 to \$227 per inventoried cow per year (24, 40). JD has lower prevalence in beef herds, but this disease still has a negative impact on trade (38, 42, 60). Concerns for human health have also been raised, since *M. avium* subsp. *paratuberculosis* has the potential to be a zoonotic and/or food-borne pathogen, as evidenced by its possible linkage to Crohn's disease (6, 8, 9, 21).

The physiology and pathogenesis of *M. avium* subsp. *paratuberculosis* have been reviewed (24, 61). Neonates and juvenile animals are the most susceptible to infection. Disease

progression is classified into four stages: silent infection and subclinical, clinical, and advanced clinical disease (61). Despite the progress made in the analysis of mechanisms of pathogenesis, a diagnostic test of high sensitivity and specificity for detection of subclinically infected animals has not been developed (15, 19, 27, 33, 34, 39, 50). In this situation, most diseased animals escape detection, especially during early infection. Likewise, current vaccines against JD are highly regulated, have poor efficacy, and interfere with diagnostic tests against bovine tuberculosis (5, 10, 20, 23, 55).

The information obtained from the completed *M. avium* subsp. *paratuberculosis* genome sequencing project ushered in the development of new tools for diagnosis and disease control (29). In the context of our study, approximately 1% of the *M. avium* subsp. *paratuberculosis* genome encodes members of the PE (Pro-Glu) and PPE (Pro-Pro-Glu) protein families, so denominated by their characteristic motifs at their N-terminal domains. These genes were initially discovered in the *Mycobacterium tuberculosis* genome, which dedicates approximately 10% of its coding capacity to these elements. Cole et al. hypothesized that the PE and PPE families may have immunological importance, being the main source of antigenic variation (14, 52, 56). This quantitative difference in coding capacity

* Corresponding author. Mailing address: 211 Veterinary Medicine and Biomedical Sciences Hall, School of Veterinary Medicine and Biomedical Sciences, University of Nebraska, Fair and East Campus Loop, Lincoln, NE 68583-0905. Phone: (402) 472-8543. Fax: (402) 472-9690. E-mail: rbarletta@unl.edu.

† Supplemental material for this article may be found at <http://cvi.asm.org/>.

∇ Published ahead of print on 17 November 2010.

seems to be rooted in the evolutionary expansion of these families as microorganisms of the *Mycobacterium tuberculosis* complex diverged from the *M. avium* group (22). *M. avium* subsp. *paratuberculosis* possesses only the ancestral members of these families. Thus, functional analyses of these proteins are significant for the development of vaccines and diagnostics, as well as for the understanding of their roles in JD pathogenesis.

This study focused on the MAP1152-MAP1156 gene cluster, as the Tn5367 transposon insertion in the colony morphology *M. avium* subsp. *paratuberculosis* strain K-10 mutant with an attenuated phenotype in bovine macrophages (31), has now been mapped ca. 0.6 kb upstream from MAP1152. To evaluate the potential role of this gene cluster in *M. avium* subsp. *paratuberculosis* immunobiology, we performed further bioinformatic analysis and determined the reactivities of MAP1152 and MAP1156 against sera from mice and rabbits immunized with live *M. avium* subsp. *paratuberculosis* and against samples from naturally infected cattle.

MATERIALS AND METHODS

Cloning, expression, and purification of *M. avium* subsp. *paratuberculosis* proteins in *Escherichia coli*. MAP1152 and MAP1156 coding sequences were amplified from *M. avium* subsp. *paratuberculosis* K-10 genomic DNA and cloned into the pMAL-c2 translational fusion expression vector using the primers 5'-ATCCTCTAGAATGGATTTTCGGGTCGTTACCGC-3' and 5'-GCGCAAGCTTCTATTTTCGGGTCGCGG-GAATG-3' for MAP1152 and 5'-ATCCTCTAG AATGAAACGGCTTTTCGAGTGTGCG-3' and 5'-GCGCAAGCTTCAGCCGG TCTCGCCCGCGGCG-3' for MAP1156. Both primer pairs amplified the corresponding full-length coding sequence. The vector and amplification products were each digested with XbaI and HindIII. Following overnight ligation at 4°C, the products were transformed into *E. coli* DH5 α and selected on LB agar plates containing 0.10 mg/ml ampicillin. Drug-resistant colonies were screened by PCR using the amplification primers, and plasmid DNA for sequencing analysis was produced from positive colonies to confirm each clone. *E. coli* protein lysates from verified clones were prepared as previously described (47). Proteins used in this study were expressed and purified as recombinant maltose-binding protein (MBP) N-terminal fusions (e.g., LacZ, MAP1152, and MAP1156; referred to here by these short names, with the understanding that all recombinant proteins used in the experiments were fusion products). These MBP-tagged recombinant proteins were overexpressed by induction of 1.0-liter LB broth cultures with 0.3 mM isopropyl- β -D-thiogalactopyranoside (Sigma Chemical Company, St. Louis, MO) for 2.5 h with shaking at 37°C. *E. coli* cells were harvested by centrifugation at 4,000 \times g and resuspended in column buffer, and the cell suspension was subjected to a freeze-thaw cycle at -20°C and sonicated under conditions described previously (1). The resulting crude extracts were purified by affinity chromatography with an amylose resin (New England Biolabs). Purified protein yields were determined from eluted fractions with a NanoDrop spectrophotometer set at 280 nm. The most concentrated fractions were pooled and dialyzed in Slide-A-Lyzer cassettes (Pierce Biotechnology Inc., Rockford, IL) immersed in 1.5 liters of phosphate-buffered saline (PBS; 150 mM NaCl, 10 mM Na₂HPO₄; pH 7.4) with three exchanges at 4°C. Purified protein aliquots were stored at -20°C. After thawing the aliquots, protein yield was reassessed by a modified Lowry assay using bovine serum albumin (BSA) as the standard. *E. coli* DH5 α harboring the parental plasmid pMAL-c2 was expressed, purified, and used as a control. Purified protein from this control strain consists of an MBP fusion (overall mass, 42 kDa) with the LacZ alpha peptide (8 kDa). Each recombinant protein was further evaluated by using GelCode blue (Pierce Biotechnology Inc., Rockford, IL)-stained SDS-PAGE gels to assess purity and expected sizes.

Electrophoresis and immunoblot analysis. Gel electrophoresis was performed using 12% (wt/vol) polyacrylamide gels. Electrophoretic transfer of proteins onto pure nitrocellulose was carried out using a TransBlot cell (Bio-Rad Laboratories, Richmond, CA) with sodium phosphate buffer (25 mM; pH 7.8) at 0.8 A for 90 min. After transfer, filters were blocked with PBS plus 2% BSA and 0.1% Tween 20 (BSA-PBST). Cattle serum samples (Table 1) were diluted 1:500 in BSA-PBST, and the rabbit and mouse sera were diluted 1:1,000. As necessary, sub-clinical (stage 2) versus clinical (stage 3) infections were assessed by fecal counts,

TABLE 1. Cattle serum samples used in the study

Serum sample	Original classification (Idexx test)	Type of infection	Source
Cow 183	+	Natural (JD)	NADC ^a
Cow 2075	+	Natural (JD)	NADC
Cow 184	+	Natural (JD)	NADC
Cow 805	+	Natural (JD)	NADC
Cow 45	+	Natural (JD)	NADC
Cow 193	-	Experimental, with <i>M. avium hominissius</i>	NADC
Cow 2291	-	Experimental, with <i>M. bovis</i> strain 95-1315	NADC
Cow 47	+	Natural (JD)	NADC
Positive control ^b	+	Natural (JD)	Idexx Laboratories
EDNA	+	Natural (JD)	NADC
Cow 308	+	Natural (JD)	NADC
2010-07	+	Natural (JD)	Nebraska dairy ^f
Negative control ^d	-	None	Idexx Laboratories
J53-90	-	None	Nebraska beef herd ^f
Cow 559	-	None	NADC
3438-08	-	None	Nebraska dairy ^f

^a NADC, National Animal Disease Center, Ames, IA.

^b Positive-control serum provided with the Idexx kit, derived from a single naturally infected Holstein cow (Idexx Technical Service).

^c Dairy or beef cattle of the University of Nebraska Lincoln Veterinary Diagnostic Center, Lincoln, NE.

^d Negative-control serum provided with the Idexx kit, derived from a single Holstein cow residing in a herd that tested negative for paratuberculosis by whole-herd testing over multiple years (Idexx Technical Service).

as described previously (62). For detection of MBP, a high-titer murine anti-MBP monoclonal antibody was diluted 1:10,000. Each blot was incubated at room temperature for 2 h with gentle rocking. After three washes in PBS plus 0.1% Tween 20, blots were incubated for 1.5 h in a horseradish peroxidase (HRP)-labeled goat anti-bovine detection antibody that was obtained from Southern Biotechnology and diluted 1:10,000 in PBS-BSA. The blots were again washed three times as described above and developed for chemiluminescence using Supersignal detection reagents (Pierce).

Quantitative analysis of band intensities on immunoblots. Band intensity was determined using the Adobe Photoshop CS4 extended application measurement tool. This version has the ability to record pixel gray values using the default measurement scale (1 pixel = 1 pixel). Each spot was measured identically by using a defined window area. Values were exported into a spreadsheet for further analysis. The background statistics were calculated by determining the means and standard deviations of the bands that had the least signal intensity within each output graph. Each intensity score was normalized to this calculated background intensity.

ELISA. An enzyme-linked immunosorbent assay (ELISA) was developed to quantify the reactivities of MAP1152 and MAP1156 proteins with a subset of serum samples from cattle with known exposure to *M. avium* subsp. *paratuberculosis* (Table 1). Antigen (0.010 mg per well) was bound to BD Falcon Pro-Bind 96-well plates overnight at 4°C. Antigen was diluted in 1.0 M sodium carbonate buffer (pH 9.8), and 0.1 ml of solution was bound in each well. After overnight incubation, the plate was washed five times with PBS and blocked with 0.3 ml BSA-PBST for 2 to 3 h at room temperature. The ELISA was performed as per the instructions provided with the HerdChek ELISA kit (Idexx Laboratories, Westbrook, ME). Briefly, sera were diluted 1:25 in either BSA-PBST or the buffer supplied by Idexx containing *Mycobacterium phlei* antigen for clarification. Diluted serum was applied (0.1 ml) to each well and incubated for 30 min at room temperature, plates were washed five times with PBS, and secondary antibody conjugate (HRP-conjugated rabbit anti-bovine IgG) was applied (0.1 ml/well) and incubated for 30 min at room temperature. After additional washing steps, 0.1 ml tetramethylbenzidine (TMB) was added, and the subsequent reaction was stopped with the supplied SDS Stop solution as the appropriate color developed. Absorbance was read at 650 nm with a Molecular Devices Vmax kinetic microplate reader and translated with the xChek software from Idexx. The sample-to-positive (S/P) ratios for each antigen were calculated based on optical density (OD) values, as follows: [(OD of serum sample - OD of negative-control serum)]/[(OD of positive-control serum - OD of negative-control serum)], as described for the Idexx HerdChek assay. Statistical analysis of ELISA results was performed using SAS 9.2 for Windows (SAS Institute Inc., Cary, NC). To compare average absorbances of all seropositive cattle samples to

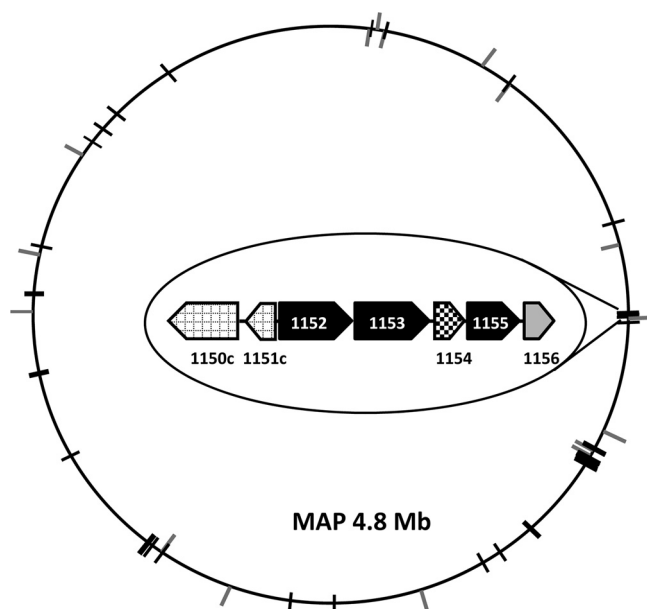


FIG. 1. Genomic map of PE, PPE, and UPF genes in *M. avium* subsp. *paratuberculosis* K-10 (MAP). Genes encoding PE (shown as bars inside of the circular chromosome), PPE (bars crossing the circular chromosome), and UPF (bars outside the circle) protein family members are shown. No PGRS protein-coding sequences were found. (Inset) MAP1152-MAP1156 genomic region, indicating genes encoding PPE proteins MAP1152, MAP1153, and MAP1155 (black boxes), UPF protein MAP1156 (gray box), hypothetical protein MAP1154 (dark patterned box), and MAP1150c and MAP1151c (light patterned boxes). Arrowed boxes indicate the direction of transcription.

the seronegative group, mixed model regression (MIXED) analysis was performed, factoring the repeated measures for day and serum sample. To evaluate within- and between-antigen serum combination differences, the generalized linear mixed models regression (GLIMMIX) analysis was used. A *P* value of <0.05 was considered significant.

RESULTS

Bioinformatic analysis of the MAP1152-MAP1156 gene cluster. Nine PE and 37 PPE protein genes are scattered around the *M. avium* subsp. *paratuberculosis* chromosome (Fig. 1). The major PPE cluster is at 1.66 Mb in the clockwise

direction in the published genome sequence (29) and comprises MAP1514, encoding a PE protein, and six PPE genes. The MAP1152-MAP1156 region of interest for this study is the second major cluster and is located 1.21 Mb in the clockwise direction. This region encodes the PPE proteins MAP1152 (40.8 kDa), MAP1153 (45.8 kDa), and MAP1155 (32.3 kDa) (Fig. 1, inset). This region also encodes a putative open reading frame (ORF) of unknown function (MAP1154; 11.8 kDa) and MAP1156 (50.7 kDa), a member of the uncharacterized protein family (UPF0089) (<http://pfam.sanger.ac.uk/family/PF03007>). The *M. avium* subsp. *paratuberculosis* genome encodes nine UPF0089 family genes, and MAP1156 is the only member that is immediately adjacent to a PPE gene (Fig. 1). This cluster does not encode a PE protein sequence.

It is tempting to speculate that genes in the MAP1152-MAP1156 region are organized in a functional unit, since ORFs further upstream and downstream are transcribed from the complementary strand with short (e.g., <200-bp) intergenic regions. However, more stringent predictions indicate that only MAP1152 and MAP1153 are organized in a true operon with an estimated probability that a pair of genes is in the same operon (pOp) value of 0.842 (<http://www.microbesonline.org/operons/gnc262316.html>) (44, 45). Nonetheless, the genes in this cluster may comprise more than one operon.

The proximal (MAP1152) and distal (MAP1156) ORFs in the cluster were selected for immunological tests of humoral immunity in infected and noninfected animals. MAP1152 encodes a typical PPE protein of 416 amino acids with a predicted molecular mass of 40.8 kDa (Table 2). Protein structure analysis predicts for the best model three *trans*-membrane helices (48; <http://www.predictprotein.org>), consistent with a surface or membrane localization, as shown for other PPE proteins (7, 25, 32, 36, 43). MAP1156 is a protein of 464 amino acids with a predicted molecular mass of 50.7 kDa. Protein structural analysis for the best fit model predicts one *trans*-membrane helix, suggesting surface localization (48). Both MAP1152 and MAP1156 have homologous sequences in both *M. avium* subsp. *paratuberculosis* and other mycobacterial genomes. Further bioinformatic analysis of the ORFs in the cluster is presented in Table 2.

TABLE 2. Characterizations of ORFs MAP1152 to MAP1156

ORF	Size (no. of aa, mass) ^a	H37Rv homolog ^b /E-value ^c	Domain, motif ^d	Comment(s) ^d
MAP1152	416, 40.7	Rv1808 (PPE32)/8.0 E-78	PPE, GxxSVPxxW	Three MH
MAP1153	454, 45.7	Rv1809 (PPE33)/1.0 E-84	PPE, GxxSVPxxW	Coding sequence starts 7 bp downstream from MAP1152; three MH
MAP1154	117, 11.7	Rv1810/8.0 E-19	DUF732 superfamily	Hypothetical protein; no MH
MAP1155	320, 32.2	Rv1807 (PPE31)/4.0 E-24	PPE, GxxSVPxxW	Attenuating mutation in <i>M. tuberculosis</i> homolog (49); two MH
MAP1156	464, 50.6	Rv1425/0.0	UPF0089	<i>M. tuberculosis</i> homolog encodes enzyme with low TGS activity (16); possibly one MH

^a Data are based on National Center for Biotechnology Information (NCBI) database output. Sizes are reported as the number of amino acids (aa) and as molecular mass (in kilodaltons).

^b Data entries based on the Pfam database (<http://pfam.sanger.ac.uk/family>). Most homologous *M. tuberculosis* proteins are not necessarily orthologs (22).

^c E-values (determined using the Blastp suite) are formatted as described in the BLAST help manual (http://www.ncbi.nlm.nih.gov/blast/blast_help.shtml).

^d MH, membrane helices (determined via the PredictProtein server [<http://www.predictprotein.org>] for protein analysis [PHDhtm output]).

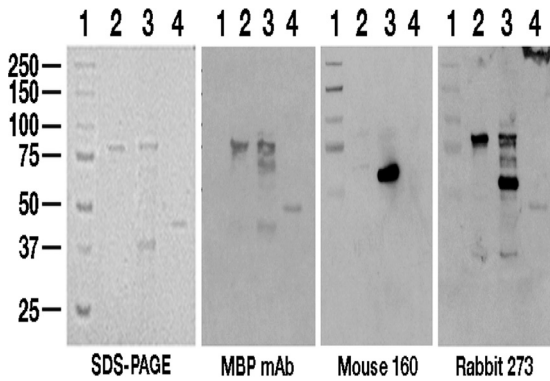


FIG. 2. SDS-PAGE and immunoblot analysis of recombinant *M. avium* subsp. *paratuberculosis* MAP1152 and MAP1156 proteins. Shown is a 12% SDS-PAGE gel, stained with GelCode blue, along with three corresponding immunoblots containing purified recombinant fusion proteins. Antibody or serum samples used to probe the immunoblot are indicated beneath the panels: MBP MAb, monoclonal antibody against the maltose-binding protein; mouse 160, serum derived from a mouse immunized with live *M. avium* subsp. *paratuberculosis* cells; rabbit 273, serum derived from a rabbit immunized with live *M. avium* subsp. *paratuberculosis* cells. Size standards, reported in kDa, are indicated to the left. Assignments for the gel and blots were as follows: lane 1, protein size standards; lane 2, MAP1152; lane 3, MAP1156; lane 4, LacZ.

Seroreactivity of recombinant proteins by immunoblot analysis. Purified recombinant proteins MAP1152 and MAP1156 were subjected to SDS-PAGE and immunoblot analyses. Equal amounts of both proteins were examined by SDS-PAGE to verify that their migration corresponded with their molecular size (Fig. 2, SDS-PAGE). Both fusion proteins migrated to the expected positions between the 75-kDa and 100-kDa protein markers, with MAP1156 (90.6 kDa) located slightly higher than MAP1152 (82.8 kDa). Likewise, LacZ (42 kDa) migrated to a position below the 50-kDa marker. These data indicate that the MBP method resulted in protein preparations of the necessary purity and yield to carry out further testing. MAP1156 did show multiple bands, in contrast to the discrete single bands observed for MAP1152 and LacZ. Immunoblot quality control analysis was also performed, using a monoclonal antibody developed to the MBP affinity tag. All three MBP fusion proteins were detected by this antibody (Fig. 2, MBP MAb). The additional bands observed in the MAP1156 preparation likely represent degradation products with the same N terminus, as the fast-migrating bands reacted also with the MBP monoclonal antibody.

The immunogenicity of the recombinant proteins was tested by immunoblotting using immune mouse (C57BL/6) or rabbit (New Zealand White) serum from animals immunized with a live preparation of *M. avium* subsp. *paratuberculosis*, as described previously (2). The mouse serum displayed little to no reactivity to MAP1152 but strong reactivity to MAP1156, with the most intense band migrating between the 50- and 75-kDa markers (Fig. 2, mouse 160). The rabbit immune serum showed strong reactivities to both proteins (Fig. 2, rabbit 273). Reactivity against the LacZ antigen carrying the MBP tag was used as a negative control. The mouse serum displayed no MBP-LacZ reactivity (Fig. 2, mouse panel, lane 4), and only a weak reaction was observed with the rabbit serum (Fig. 2,

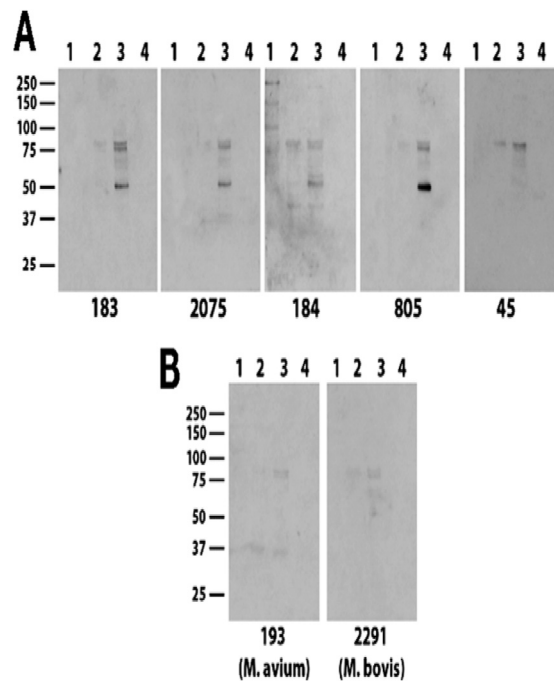


FIG. 3. Western blot analysis of antibody responses to MAP1152 and MAP1156 in naturally infected cattle. Immunoblots containing MAP1152 and MAP1156 were probed with sera from five cows (183, 2075, 84, 805, and 45) naturally infected with *M. avium* subsp. *paratuberculosis* (A) or from two additional cows experimentally infected with *M. avium* or *M. bovis* (B). Size standards, reported in kDa, are indicated to the left. Assignments for the blots were as follows: lane 1, protein size standards; lane 2, MAP1152; lane 3, MAP1156; lane 4, LacZ.

rabbit panel, lane 4). Thus, the MBP tag yielded no to minimal reactivity in these immunoblot assays.

Immunoblot assays were also performed with sera from five cattle naturally infected with *M. avium* subsp. *paratuberculosis* (Fig. 3A, 183, 2075, 184, 805, and 45). MAP1156 (Fig. 3A, lane 3, all panels) showed higher levels of reactivity than MAP1152 (Fig. 3A, lane 2, all panels). Furthermore, densitometry analysis (see Table S1 in the supplemental material) enabled a semiquantitative comparison and showed that MAP1156 displayed 2- to 5-fold more seroreactivity than MAP1152 among these *M. avium* subsp. *paratuberculosis*-seropositive samples. Conversely, weak reactivity was observed with sera from cattle experimentally infected with *M. avium* or *M. bovis* (Fig. 3B). None of the serum samples yielded any background activity against the LacZ antigen or the MBP tag (Fig. 3, lane 4, each panel).

We also followed the reactivity of the proteins against serum samples taken at different time points during natural infection. Samples corresponded to bleeds taken 9 to 14 months apart, corresponding to disease progression from subclinical to clinical infection. Results obtained with these samples (Fig. 4) indicated that MAP1152 did not react with any of the serum samples (Fig. 4, upper panel, lanes 1 to 4), while MAP1156 (Fig. 4, middle panel, lanes 1 to 4) and *M. avium* subsp. *paratuberculosis* K-10 whole-cell extract (Fig. 4, lower panel) displayed increasing reactivities with samples from the subclinical (Fig. 4, lanes 1 and 2) and clinical stages (Fig. 4, lanes 3 and 4).

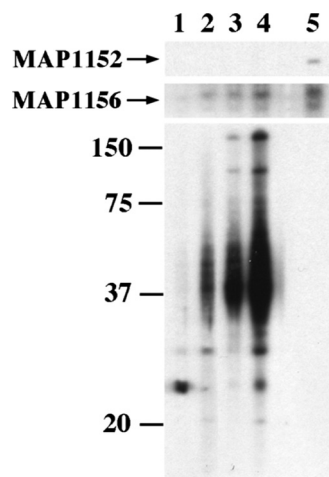


FIG. 4. Western blot analysis of antibody responses to MAP1152 and MAP1156 during the course of JD. Immunoblots of MAP1152 (upper gel), MAP1156 (middle gel), and K-10 whole-cell extract (lower gel) were probed with serum samples withdrawn from a naturally infected cow (cow 47) at various times during the course of the experiment: lane 1, first bleed, subclinical infection; lane 2, 12 months after first bleed, borderline clinical/subclinical infection; lane 3, 26 months after first bleed, clinical infection; lane 4, 35 months after first bleed, advanced clinical infection; lane 5, anti-MBP monoclonal antibody control. Size standards (in kDa) are indicated to the left.

Both proteins reacted with the anti-MBP monoclonal antibody control (Fig. 4, lane 5), although MAP1152 yielded a weaker reaction.

Seroreactivity of recombinant protein with sera from *M. avium* subsp. *paratuberculosis*-infected and noninfected cattle by ELISA. As the ELISA technology is readily adaptable to diagnostic applications, we also determined the reactivities of MAP1152 and MAP1156 by this method. In addition, this assay is generally performed to evaluate the antigen-antibody reaction in the absence of denaturing agents. Thus, both linear and conformational epitopes may contribute to the overall reactivity. Due to limiting amounts of serum samples, the ELISA was performed using archived serum samples which were previously evaluated with the Idexx test at the University of Nebraska—Lincoln Veterinary Diagnostic Laboratory (Table 1).

Each sample was tested in triplicate against LacZ (negative-control antigen) and on three different days in duplicate (day 3) or triplicate (days 1 and 2) to evaluate reproducibility and performance against MAP1152, MAP1156, and a standard *M. avium* subsp. *paratuberculosis* antigen control (the Idexx antigen, a proprietary mixture of *M. avium* subsp. *paratuberculosis* antigens) included in the Idexx test kit (see Table S2 in the supplemental material). Each antigen showed low reactivity and low variability as tested against seronegative serum samples from noninfected cattle. As expected, the differences in mean absorbance values for samples from *M. avium* subsp. *paratuberculosis*-infected versus noninfected cattle were statistically significant for MAP1152 ($P \leq 0.01$), MAP1156 ($P \leq 0.05$), and the Idexx antigen ($P \leq 0.001$), with more variable results for MAP1156 and the Idexx antigen (see Table S3 in the supplemental material). In contrast, the difference in absorbance means was not significant for the LacZ negative-control

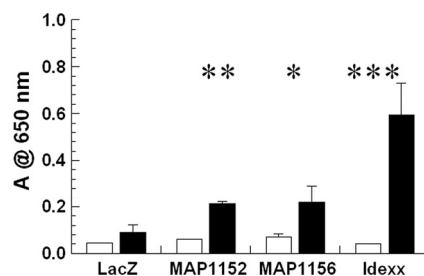


FIG. 5. Seroreactivities of MAP1152 and MAP1156 recombinant proteins to infected and noninfected cattle. Antigen (0.010 mg) reactivity was evaluated by ELISA against sera from cattle naturally infected with *M. avium* subsp. *paratuberculosis* (filled bars) or sera from culture-negative cattle (open bars). Each serum sample was diluted 1:25 in Idexx dilution buffer. Each column represents mean absorbance (from triplicate measurements against LacZ; averaged from measurements on three different days in duplicate or triplicate for other antigens [see Table S2 of the supplemental material]) per antigen, \pm standard errors of the means from noninfected cattle (left columns) or infected cattle (right columns), as evidenced from the original classification of serum samples. Significance levels are indicated as follows: *, $P \leq 0.05$; **, $P \leq 0.01$; ***, $P \leq 0.001$.

antigen carrying the MBP tag ($P > 0.05$). However, the reactivity of seropositive samples against LacZ was also more variable, as indicated by the error bars in Fig. 5. With the *M. avium* subsp. *paratuberculosis* capture antigens we were able to differentiate, in the combined analysis, between the groups of seropositive and seronegative samples. Thus, *M. avium* subsp. *paratuberculosis* infection results in a humoral response directed against epitopes present in MAP1152, MAP1156, and the Idexx antigen. However, absorbance values obtained using MAP1152 and MAP1156 as the capture antigens were lower than those attained with the Idexx capture antigen. This performance is not surprising, because these results were obtained with the standardized Idexx test protocol.

Comparative analysis of the reactivity of each serum-antigen combination was also carried out (Fig. 6). Reactivity trends were similar for both MAP1152 and MAP1156, as all samples with higher absorbance readings for MAP1152 also yielded higher values for MAP1156. The Idexx antigen followed a similar trend, except for the positive control, as all three *M. avium* subsp. *paratuberculosis* antigens yielded similar absorbance values. In contrast, three seropositive samples (EDNA, 308, and 2010-07) yielded significantly higher absorbance values for the Idexx antigen than for MAP1152 and MAP1156. No samples were expected to yield above-background absorbance readings with LacZ, the negative antigen control carrying the MBP tag. However, the EDNA serum sample displayed approximately four-times-higher absorbance readings than any other sample.

Both statistical analysis using GLIMMIX and calculation of S/P ratios for the Idexx antigen yielded the same classification as the original test (see Tables S2 and S4 in the supplemental material). Because cutoff values for S/P ratios are dependent on the particular assay procedure, capture antigen, and selection of an appropriate positive-control serum, GLIMMIX provides the more accurate analysis for the recombinant antigens. Absorbance means for each antigen-serum combination were compared to each other, and samples were classified as positive

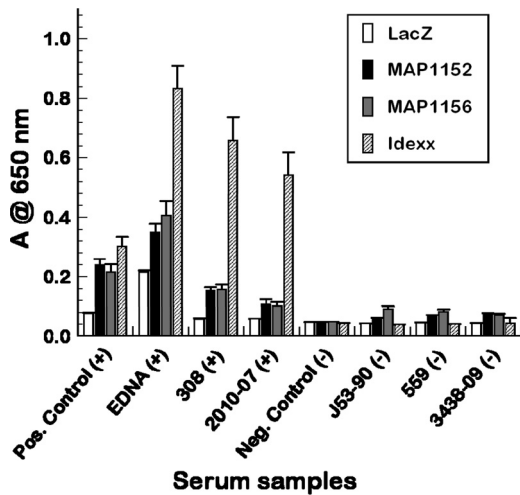


FIG. 6. Individual responses of serum samples from infected and noninfected cattle to recombinant antigens. Antigen (0.010 mg) reactivity was evaluated by ELISA against sera from cattle naturally infected with *M. avium* subsp. *paratuberculosis* and sera from culture-negative cattle. Each serum was diluted 1:25 in Idexx dilution buffer. Each column represents mean absorbance (triplicate measurements against LacZ; average measurements on three different days in duplicate or triplicate for other antigens, as indicated in Table S2 of the supplemental material) per antigen, \pm standard errors of the means from noninfected (–) or infected (+) cattle, as evidenced from the original classification of serum samples. The reaction to each antigen is indicated (see inset for pattern key).

or negative based on the *P* value obtained for the comparison against the negative-control serum for the corresponding test antigen. This analysis indicated that the nonspecific MBP-LacZ antigen control identified all samples, except EDNA, as seronegative; in contrast, antigens MAP1152 and MAP1156 misclassified only the seropositive sample 2010-07 as seronegative (see Table S4). Thus, overall, all *M. avium* subsp. *paratuberculosis* antigens yielded a classification of serum samples consistent with the original test.

DISCUSSION

Development of effective strategies for the control of JD remains one of the most challenging issues in animal health (15, 19). Advances in *M. avium* subsp. *paratuberculosis* genomics and molecular genetics provide an integrated rational approach to solve this problem (1, 3, 29). In this context, the search for new diagnostic tests can be most effective if combined with novel approaches to vaccination and knowledge of what the test indicates regarding the underlying mechanisms of disease pathogenesis. Targeting of the MAP1152-MAP1156 gene cluster was based on the identification of an attenuating mutation possibly related to the expression of this cluster and a potential role of the encoded proteins as B- or T-cell antigens. An attenuated mutant may serve as a candidate live attenuated vaccine strain and the protein as a subunit vaccine or diagnostic indicator; all relevant aspects are combined into an integrated approach.

In this study, we demonstrated that both MAP1152 and MAP1156 encode reactive B-cell epitopes, a result predicted from the surface localization implied by *in silico* analysis (Table

2). This finding is also consistent with prior experimental evidence on other PE/PPE proteins. For example, the *M. tuberculosis* protein Rv2430c (PE25) was identified as a strong B-cell antigen (12), and the seroreactivity of MAP3420 c was demonstrated in cattle (36). In contrast, antigens MAP1518 (Map41; ortholog of Rv1808 [PPE32]) and MAP3184 (Map39; ortholog of Rv3135 [PPE50]), the *M. avium* strain 104 MaPE protein, and the cell wall-associated *M. tuberculosis* protein Rv3873 (PPE68) serve as T-cell antigens (35, 37, 41).

MAP1152 and related PPE proteins MAP1153 and MAP1155 are members of the ancestral PPE sublineage IV (22). The genes encoding these proteins belong to an ancestral cluster that underwent duplication events from ancestral ESAT-6 clusters but without a concomitant duplication of the ESAT-6 genes and, thus, these paralogs are no longer associated with the ESAT-6 genes. PE/PPE genes are usually organized in operons encompassing at least several PE and/or PPE members (46, 58). Biochemical evidence indicates that PE and PPE function in pairwise combinations of interacting proteins exposed to the cell surface (18, 46, 54), with the larger-sized PPE proteins providing a pocket for the PE partner (54). However, MAP1152 is organized in a cluster devoid of coding sequences for PE proteins. Because the probability of PPE proteins participating in pairwise associations decreases for unlinked PE and PPE genes (46), the function of MAP1152 may or may not require a PE partner. Instead, MAP1152 may play additional roles in the mechanisms of pathogenesis, as shown for other PE/PPE proteins. For example, *M. tuberculosis* transposon mutants of the PE/PPE genes Rv1807 (PPE31), Rv3872 (PPE35), and Rv3873 (PPE68) are attenuated in mice (49). Likewise, a transposon mutant in the *M. avium* PPE gene homologous to Rv1787 (PPE25) displayed impaired growth in macrophages, reduced virulence in mice, and failed to prevent phagosome acidification (26, 30). Thus, a group of PE and PPE proteins may be necessary for intracellular survival.

MAP1156 is also a B-cell antigen, with stronger reactivity than MAP1152 in Western blot assays, a property also consistent with its reactivity with immune mouse and rabbit sera and inferred surface localization. MAP1156 belongs to the uncharacterized protein family UPF0089. *M. tuberculosis* encodes 15 members of this family, which includes proteins with triacylglycerol synthase (TGS) activity (16). The *M. tuberculosis* ORF Rv1425 is the closest homolog to MAP (Table 2), but this ORF has been shown not to possess significant TGS activity, at least under the conditions tested. One possible role consistent with a strong humoral reaction is that this ORF “hitchhiked” with *M. avium* subsp. *paratuberculosis* into a coexpression unit that modulates the immune response. Microorganisms of the *M. tuberculosis* complex possess a large number of PE-PGRS proteins that are associated with immunoregulatory roles (4, 17). However, as indicated above, the *M. avium* subsp. *paratuberculosis* evolutionary lineage separated prior to the further expansion of the ESAT-6 region V that gave rise to the PE-PGRS and PPE-MPTR sublineage V PE/PPE proteins (22). Thus, the absence of PE-PGRS proteins may require the recruitment of other proteins, for example, MAP1156, to play this immunomodulatory role. Future experiments will be directed to identify T-cell epitopes in both MAP1152 and MAP1156. These tests are indispensable for determining the major roles of these antigens in immunopathogenesis. For

example, it is possible that the PPE protein MAP1152, the weaker B-cell antigen in Western immunoblotting analyses, may elicit a predominant T-cell response early in infection, with MAP1156 exerting a countermodulating B-cell response, most favorable for *M. avium* subsp. *paratuberculosis* to maintain a chronic infection. This hypothesis is consistent with the increasing MAP1156 seroreactivity observed with serum samples withdrawn as JD progressed from the subclinical to clinical stage (Fig. 4). However, a more detailed study of linear and conformational epitopes in these proteins, especially for MAP1152, should be undertaken, as conformational epitopes may not be reactive in Western immunoblot assays.

The B-cell reactivities of both MAP1152 and MAP1156 in Western blot assays and the ELISA with serum samples from *M. avium* subsp. *paratuberculosis*-infected cattle are likely associated with private rather than cross-reactive or shared epitopes from related *M. avium* subsp. *paratuberculosis* proteins. In this context, the closest paralog to MAP1152 is MAP1518, with 47% identity. Likewise, the closest paralog to MAP1156 is MAP1969c, with 38% identity (see Table S5 in the supplemental material). The low degree of reactivity of MAP1152 in the immunoblot assays against sera from *M. bovis*-infected animals may be explained in a similar manner, as the closest homolog (Mb1837) shares only 50% identity. In contrast, the low reactivity of MAP1156 against the *M. bovis* serum, and of MAP1152 and MAP1156 against *M. avium hominissuis* serum, may be associated with low expression levels in these microorganisms. Otherwise, the corresponding proteins are highly homologous, with 86 to 99% identity (see Table S5) and, thus, likely to be highly cross-reactive, as most epitopes are shared. Moreover, the MAP1152-MAP1156 cluster organization is conserved between *M. avium* subsp. *paratuberculosis* and *M. avium* 104 (a sequenced isolate of *M. avium* subsp. *hominissuis*), with both genomes possessing highly homologous genes within this region. However, sequence divergence with *M. avium* 104 occurs upstream from MAP1152 that could affect gene regulation. Nonetheless, to substantiate these findings for the development of diagnostic tests, it will be necessary to test a larger group of cattle infected with *M. bovis*, *M. avium* subspecies, and other environmental species, such as *Mycobacterium kansasii*.

Interestingly, MAP1152, MAP1156, and the Idexx antigen yielded similar absorbance values against the standardized Idexx positive-control bovine serum included in the Idexx kit, which is from a single naturally infected Holstein cow (Table 1). However, the other three seropositive clinical samples reacted more strongly with the Idexx antigen (Fig. 6). As indicated above, these results may be due to methodological aspects, as the overall assay optimization was based on the Idexx protocol. Alternatively, or by compounding effects, the increased reactivity in these samples against the Idexx antigen may in part reflect the presence of cross-reactive antibodies against the various *M. avium* subsp. *paratuberculosis* proteins present in the Idexx antigen.

In summary, *M. avium* subsp. *paratuberculosis*-infected cattle mount a humoral response to both MAP1152 and MAP1156. Further research is needed to determine the values of these recombinant proteins as diagnostic capture antigens, subunit vaccines, markers of disease progression, and their suitability for the development of tests for diagnosis of infected from

vaccinated animals (DIVA), coupled with the development of live attenuated deletion mutant marker vaccines (13, 59).

ACKNOWLEDGMENTS

This work was supported by funds from the Johne's Disease Integrated Program (J.P.B. and R.G.B.) and USDA-ARS (J.P.B.), USDA grant CSREES-NRI 2004-35204-14231 (R.G.B. and C.J.C.), the BARD program grant IS-3673-05C (R.G.B.), USDA Animal Health Project NEB14-141 (R.G.B.), and the Department of Veterinary and Biomedical Sciences at the University of Nebraska (D.R.S., D.S.M., and R.G.B.).

We thank Malory Becker for her assistance to A.L.P. in preparation of materials and reagents. We thank Steve Kachman for assistance with SAS analysis.

REFERENCES

- Bannantine, J. P., and M. L. Paustian. 2006. Identification of diagnostic proteins in *Mycobacterium avium* subspecies *paratuberculosis* by a whole genome analysis approach. *Methods Mol. Biol.* **345**:185–196.
- Bannantine, J. P., and J. R. Stabel. 2001. Identification of two *Mycobacterium avium* subspecies *paratuberculosis* gene products differentially recognized by sera from rabbits immunised with live mycobacteria but not heat-killed mycobacteria. *J. Med. Microbiol.* **50**:795–804.
- Bannantine, J. P., et al. 2008. Development and use of a partial *Mycobacterium avium* subspecies *paratuberculosis* protein array. *Proteomics* **8**:463–474.
- Banu, S., et al. 2002. Are the PE-PGRS proteins of *Mycobacterium tuberculosis* variable surface antigens? *Mol. Microbiol.* **44**:9–19.
- Begg, D. J., and J. F. T. Griffin. 2005. Vaccination of sheep against *M. paratuberculosis*: immune parameters and protective efficacy. *Vaccine* **23**:4999–5008.
- Bernstein, C. N., J. F. Blanchard, P. Rawsthorne, and M. T. Collins. 2004. Population-based case control study of seroprevalence of *Mycobacterium paratuberculosis* in patients with Crohn's disease and ulcerative colitis. *J. Clin. Microbiol.* **42**:1129–1135.
- Bottai, D., and R. Brosch. 2009. Mycobacterial PE, PPE and ESX clusters: novel insights into the secretion of these most unusual protein families. *Mol. Microbiol.* **73**:325–328.
- Chacon, O., L. E. Bermudez, and R. G. Barletta. 2004. Johne's disease, inflammatory bowel disease, and *Mycobacterium paratuberculosis*. *Annu. Rev. Microbiol.* **58**:329–363.
- Chamberlin, W., G. Ghobrial, M. Chehtane, and S. A. Naser. 2007. Successful treatment of a Crohn's disease patient infected with bacteremic *Mycobacterium paratuberculosis*. *Am. J. Gastroenterol.* **102**:689–691.
- Chen, L. H., et al. 2008. Immune responses in mice to *Mycobacterium avium* subsp. *paratuberculosis* following vaccination with a novel 74F recombinant polyprotein. *Vaccine*. **26**:1253–1262.
- Chiodini, R. J., H. J. Van Kruiningen, and R. S. Merkal. 1984. Ruminant paratuberculosis (Johne's disease): the current status and future prospects. *Cornell Vet.* **74**:218–262.
- Choudhary, R. K., et al. 2003. PPE antigen Rv2430c of *Mycobacterium tuberculosis* induces a strong B-cell response. *Infect. Immun.* **71**:6338–6343.
- Cirillo, J. D., C. K. Stover, B. R. Bloom, W. R. Jacobs, Jr., and R. G. Barletta. 1995. Bacterial vaccine vectors and bacillus Calmette-Guerin. *Clin. Infect. Dis.* **20**:1001–1009.
- Cole, S. T., et al. 1998. Deciphering the biology of *Mycobacterium tuberculosis* from the complete genome sequence. *Nature* **393**:537–544.
- Collins, M. T., et al. 2005. Evaluation of five antibody detection tests for diagnosis of bovine paratuberculosis. *Clin. Diagn. Lab. Immunol.* **12**:685–692.
- Daniel, J., et al. 2004. Induction of a novel class of diacylglycerol acyltransferases and triacylglycerol accumulation in *Mycobacterium tuberculosis* as it goes into a triacylglycerol state in culture. *J. Bacteriol.* **186**:5017–5030.
- Delogu, G., and M. J. Brennan. 2001. Comparative immune response to PE and PE_PGRS antigens of *Mycobacterium tuberculosis*. *Infect. Immun.* **69**:5606–5611.
- Delogu, G., et al. 2004. Rv1818c-encoded PE_PGRS protein of *Mycobacterium tuberculosis* is surface exposed and influences bacterial cell structure. *Mol. Microbiol.* **52**:725–733.
- Eda, S., et al. 2005. New method of serological testing for *Mycobacterium avium* subsp. *paratuberculosis* (Johne's disease) by flow cytometry. *Foodborne Pathog. Dis.* **2**:250–262.
- Emery, D. L., and R. J. Whittington. 2004. An evaluation of mycophage therapy, chemotherapy and vaccination for control of *Mycobacterium avium* subsp. *paratuberculosis* infection. *Vet. Microbiol.* **104**:143–155.
- Feller, M., et al. 2007. *Mycobacterium avium* subspecies *paratuberculosis* and Crohn's disease: a systematic review and meta-analysis. *Lancet Infect. Dis.* **7**:607–613.

22. Gey van Pittius, N. C., et al. 2006. Evolution and expansion of the *Mycobacterium tuberculosis* PE and PPE multigene families and their association with the duplication of the ESAT-6 (esx) gene cluster regions. *BMC Evol. Biol.* **6**:95.
23. Groenendaal, H., and D. T. Galligan. 2003. Economic consequences of control programs for paratuberculosis in midsize dairy farms in the United States. *J. Am. Vet. Med. Assoc.* **223**:1757–1763.
24. Harris, N. B., and R. G. Barletta. 2001. *Mycobacterium avium* subsp. *paratuberculosis* in veterinary medicine. *Clin. Microbiol. Rev.* **14**:489–512.
25. He, Z., and J. De Buck. 2010. Localization of proteins in the cell wall of *Mycobacterium avium* subsp. *paratuberculosis* K10 by proteomic analysis. *Proteome Sci.* **8**:21.
26. Jha, S. S., et al. 2010. Virulence-related *Mycobacterium avium* subsp. *hominissuis* MAV_2928 gene is associated with vacuole remodeling in macrophages. *BMC Microbiol.* **10**:100.
27. Kalis, C. H., M. T. Collins, J. W. Hesselink, and H. W. Barkema. 2003. Specificity of two tests for the early diagnosis of bovine paratuberculosis based on cell-mediated immunity: the Johnin skin test and the gamma interferon assay. *Vet. Microbiol.* **97**:73–86.
28. Lambrecht, R. S., J. F. Carriere, and M. T. Collins. 1988. A model for analyzing growth kinetics of a slowly growing *Mycobacterium* sp. *Appl. Environ. Microbiol.* **54**:910–916.
29. Li, L., et al. 2005. The complete genome sequence of *Mycobacterium avium* subspecies *paratuberculosis*. *Proc. Natl. Acad. Sci. U. S. A.* **102**:12344–12349.
30. Li, Y., E. Miltner, M. Wu, M. Petrofsky, and L. E. Bermudez. 2005. A *Mycobacterium avium* PPE gene is associated with the ability of the bacterium to grow in macrophages and virulence in mice. *Cell. Microbiol.* **7**:539–548.
31. Livneh, A., et al. 2007. In vivo and in vitro characterization of *Mycobacterium avium* subsp. *paratuberculosis* (MAP) mutants, p. 108–114. In E. J. B. Manning and S. S. Nielsen (ed.), *Proceedings of the 8th International Colloquium on Paratuberculosis*. International Association of Paratuberculosis, Madison, WI.
32. McEvoy, C. R., P. D. van Helden, R. M. Warren, and N. C. Gey van Pittius. 2009. Evidence for a rapid rate of molecular evolution at the hypervariable and immunogenic *Mycobacterium tuberculosis* PPE38 gene region. *BMC Evol. Biol.* **9**:237.
33. McKenna, S. L., et al. 2005. Comparison of two enzyme-linked immunosorbent assays for diagnosis of *Mycobacterium avium* subsp. *paratuberculosis*. *J. Vet. Diagn. Invest.* **17**:463–466.
34. McKenna, S. L. B., G. P. Keefe, H. W. Barkema, and D. C. Sockett. 2005. Evaluation of three ELISAs for *Mycobacterium avium* subsp. *paratuberculosis* using tissue and fecal culture as comparison standards. *Vet. Microbiol.* **110**:105–111.
35. Nagata, R., Y. Muneta, K. Yoshihara, Y. Yokomizo, and Y. Mori. 2005. Expression cloning of gamma interferon-inducing antigens of *Mycobacterium avium* subsp. *paratuberculosis*. *Infect. Immun.* **73**:3778–3782.
36. Newton, V., S. L. McKenna, and J. De Buck. 2009. Presence of PPE proteins in *Mycobacterium avium* subsp. *paratuberculosis* isolates and their immunogenicity in cattle. *Vet. Microbiol.* **135**:394–400.
37. Okkels, L. M., et al. 2003. PPE protein (Rv3873) from DNA segment RD1 of *Mycobacterium tuberculosis*: strong recognition of both specific T-cell epitopes and epitopes conserved within the PPE family. *Infect. Immun.* **71**:6116–6123.
38. Osterstock, J. B., G. T. Fosgate, N. D. Cohen, J. N. Derr, and A. J. Roussel. 2008. Familial and herd-level associations with paratuberculosis enzyme-linked immunosorbent assay status in beef cattle. *J. Anim. Sci.* **86**:1977–1983.
39. Osterstock, J. B., et al. 2007. Contribution of environmental mycobacteria to false-positive serum ELISA results for paratuberculosis. *J. Am. Vet. Med. Assoc.* **230**:896–901.
40. Ott, S. L., S. J. Wells, and B. A. Wagner. 1999. Herd-level economic losses associated with Johne's disease on US dairy operations. *Prev. Vet. Med.* **40**:179–192.
41. Parra, M., N. Cadieux, T. Pickett, V. Dheenadhayalan, and M. J. Brennan. 2006. A PE protein expressed by *Mycobacterium avium* is an effective T-cell immunogen. *Infect. Immun.* **74**:786–789.
42. Pearce, B. H., et al. 2008. Comparison of three methods of surveillance with application to the detection of Johne's disease seropositivity in Texas cattle. *Prev. Vet. Med.* **86**:1–7.
43. Plotkin, J. B., J. Dushoff, and H. B. Fraser. 2004. Detecting selection using a single genome sequence of *M. tuberculosis* and *P. falciparum*. *Nature* **428**:942–945.
44. Price, M. N., E. J. Alm, and A. P. Arkin. 2005. Interruptions in gene expression drive highly expressed operons to the leading strand of DNA replication. *Nucleic Acids Res.* **33**:3224–3234.
45. Price, M. N., K. H. Huang, E. J. Alm, and A. P. Arkin. 2005. A novel method for accurate operon predictions in all sequenced prokaryotes. *Nucleic Acids Res.* **33**:880–892.
46. Riley, R., M. Pellegrini, and D. Eisenberg. 2008. Identifying cognate binding pairs among a large set of paralogs: the case of PE/PPE proteins of *Mycobacterium tuberculosis*. *PLoS Comput. Biol.* **4**:e1000174.
47. Rockey, D. D., and J. L. Rosquist. 1994. Protein antigens of *Chlamydia psittaci* present in infected cells but not detected in the infectious elementary body. *Infect. Immun.* **62**:106–112.
48. Rost, B., G. Yachdav, and J. Liu. 2004. The PredictProtein server. *Nucleic Acids Res.* **32**:W321–W326.
49. Sassetti, C. M., and E. J. Rubin. 2003. Genetic requirements for mycobacterial survival during infection. *Proc. Natl. Acad. Sci. U. S. A.* **100**:12989–12994.
50. Semret, M., C. Y. Turenne, and M. A. Behr. 2006. Insertion sequence IS900 revisited. *J. Clin. Microbiol.* **44**:1081–1083.
51. Stabel, J. R. 1998. Johne's disease: a hidden threat. *J. Dairy Sci.* **81**:283–288.
52. Stinear, T. P., et al. 2008. Insights from the complete genome sequence of *Mycobacterium marinum* on the evolution of *Mycobacterium tuberculosis*. *Genome Res.* **18**:729–741.
53. Stott, A. W., G. M. Jones, R. W. Humphry, and G. J. Gunn. 2005. Financial incentive to control paratuberculosis (Johne's disease) on dairy farms in the United Kingdom. *Vet. Rec.* **156**:825–831.
54. Strong, M., et al. 2006. Toward the structural genomics of complexes: crystal structure of a PE/PPE protein complex from *Mycobacterium tuberculosis*. *Proc. Natl. Acad. Sci. U. S. A.* **103**:8060–8065.
55. Sweeney, R. W., et al. 2009. Effect of subcutaneous administration of a killed *Mycobacterium avium* subsp. *paratuberculosis* vaccine on colonization of tissues following oral exposure to the organism in calves. *Am. J. Vet. Res.* **70**:493–497.
56. Tekaiia, F., et al. 1999. Analysis of the proteome of *Mycobacterium tuberculosis* in silico. *Tuber. Lung Dis.* **79**:329–342.
57. Tiwari, A., et al. 2007. Production effects of pathogens causing bovine leukosis, bovine viral diarrhea, paratuberculosis, and neosporosis. *J. Dairy Sci.* **90**:659–669.
58. Tundup, S., Y. Akhter, D. Thiagarajan, and S. E. Hasnain. 2006. Clusters of PE and PPE genes of *Mycobacterium tuberculosis* are organized in operons: evidence that PE Rv2431c is co-transcribed with PPE Rv2430c and their gene products interact with each other. *FEBS Lett.* **580**:1285–1293.
59. Vordermeier, M., S. V. Gordon, and A. R. Hewinson. 2009. Antigen mining to define *Mycobacterium bovis* antigens for the differential diagnosis of vaccinated and infected animals: a VLA perspective. *Transbound. Emerg. Dis.* **56**:240–247.
60. Wells, J. E., et al. 2009. Prevalence of *Mycobacterium avium* subsp. *paratuberculosis* in ileocecal lymph nodes and on hides and carcasses from cull cows and fed cattle at commercial beef processing plants in the United States. *J. Food Prot.* **72**:1457–1462.
61. Whitlock, R. H., and C. Buergelt. 1996. Preclinical and clinical manifestations of paratuberculosis (including pathology). *Vet. Clin. North Am. Food Anim. Pract.* **12**:345–356.
62. Whitlock, R. H., S. J. Wells, R. W. Sweeney, and J. Van Tiem. 2000. ELISA and fecal culture for paratuberculosis (Johne's disease): sensitivity and specificity of each method. *Vet. Microbiol.* **77**:387–398.